Caractérisation physico-chimique de phytolithes de bambous (Nastus borbonicus)

I. INTRODUCTION

L'étude du cycle global du silicium (Si) n'est pas nouvelle. En effet, depuis les années 1960 de nombreuses études ont été consacrées à la caractérisation de ce cycle. Cependant, ce n'est que depuis quelques années seulement que l'importance du cycle biogéochimique de cet élément a été mise en avant dans les environnements superficiels continentaux.

Avant son transfert aux océans par l'intermédiaires des rivières, l'acide silicique dissous présent dans les solutions interstitielles peut se trouver piéger par les racines des plantes et être ensuite précipité dans les cellules des tissus sous formes de microparticules d'opales appelées phytolithes. Ils pourront être ensuite libérés dans les litières et transférés aux sols ou évacués par voies aériennes ou hydrographiques après dégradation des matières organiques. Il a été montré que la dissolution de ces phytolithes en milieu tropical pouvait contribuer jusqu'à 3 fois plus que la dissolution des minéraux silicatés non biogéniques aux flux de silice dissoute exportés hors du profil d'altération.

La prise en compte de ce recyclage du silicium par les plantes ne peut donc pas être écartée mais est actuellement limitée par le manque de données physico-chimiques de base sur les phytolithes.

Le but de ce travail va donc être d'acquérir ces données essentielles afin de mieux quantifier ce cycle biogéochimique du silicium et par conséquent de mieux contraindre le cycle global du silicium. Pour ce faire, plusieurs techniques complémentaires vont être mises en œuvre et appliqués sur des phytolithes de bambous provenant de l'île de la Réunion.

II. RESUME EN FRANÇAIS DE L'ARTICLE : " SURFACE PROPERTIES, SOLUBILITY AND DISSOLUTION KINETICS OF BAMBOO PHYTOLITHS "

Comme nous l'avons vu, de nombreuses études ont montré que les phytolithes, constitués essentiellement d'opale micrométrique, ont manifestement un contrôle important sur le cycle du silicium dans les environnements terrestres continentaux superficiels. Cependant, les propriétés thermodynamiques et la réactivité dans les solutions aqueuses de ces phytolithes sont encore peu connues.

Le but de se travail va donc être de déterminer la solubilité et les vitesses de dissolution de phytolithes de bambous collectés sur l'île de la Réunion et de caractériser leurs propriétés surfaciques via des mesures électrophorétiques et des titrages potentiométriques dans une large gamme de pH. Ainsi, le produit de solubilité des phytolithes de « sol » déterminé à 25 °C (pK^0_{sp} = 2.74) est équivalent à celui d'une silice vitreuse et est 17 fois plus grand que celui du quartz. D'autre part, l'enthalpie de la réaction de dissolution des phytolithes déterminée entre 25 et 80°C ($\Delta H_r^{25\text{-}80°C}$ = 10.85 kJ/mol) est proche de celle de la silice amorphe mais significativement plus faible que celle du quartz. Les mesures électrophorétiques ont permis de déterminer le pH au point isoélectrique (pH_{IEP}) pour les phytolithes de « sol » et « chauffés » (chauffage à 450°C pour détruire la matière organique). Ce pH_{IEP} est respectivement de 1.2 ± 0.1 et de 2.5 ± 0.2 pour les phytolithes de « sol » et les phytolithes « chauffés », et il correspond au pH pour lequel la surface du phytolithes aura autant de sites surfaciques chargés négativement que de sites chargés positivement. Les titrages acido-basiques de la surface de ces phytolithes ont permis de générer un modèle de complexation surfacique (SCM) à 2 pK. En ce qui concerne les vitesses de dissolution des phytolithes, qui ont été mesurées dans des réacteurs mixed-flow, loin de l'équilibre et dans une gamme de pH allant de 2 à 12, elles se trouvent être intermédiaires entre celles du quartz et celles de la silice vitreuse. La dépendance au pH de ces vitesses de dissolution (R) a été

modélisée selon le concept de la théorie de coordination surfacique en utilisant l'équation suivante :

$$R = k_1 \cdot \{>SiOH_2^+\}^n + k_2 \cdot \{>SiOH^0\} + k_3 \cdot \{>SiO^-\}^m$$

où {>i} correspond à la concentration des espèces surfaciques présentent à l'interface SiO_2-H_2O, k_i sont les constantes des trois réactions parallèles et *n* et *m* représentent respectivement l'ordre des réactions de protonation et de déprotonation.

Les données acquises tout au long de ce travail montrent que les vitesses de dissolution des phytolithes présentent un minimum à un pH de 3 environ. Ces résultats peuvent donc expliquer leur bonne préservation dans les horizons des sols acides de l'île de la Réunion. Si on raisonne en terme de cycle biogéochimique du silicium, les phytolithes peuvent donc représenter un vaste réservoir de stockage de silicium, qui peut jouer par conséquent un rôle majeur dans la régulation des flux de silice dissoute dans les environnements aquatiques terrestres.

III. SURFACE PROPERTIES, SOLUBILITY AND DISSOLUTION KINETICS OF BAMBOO PHYTOLITHS

Available online at www.sciencedirect.com
SCIENCE DIRECT®
Geochimica et Cosmochimica Acta 70 (2006) 1939–1951
Geochimica
www.elsevier.com/locate/gca

Surface properties, solubility and dissolution kinetics of bamboo phytoliths

Fabrice Fraysse [a,*], Oleg S. Pokrovsky [a,*], Jacques Schott [a], Jean-Dominique Meunier [b]

[a] LMTG (Experimental Geochemistry and Biogeochemistry), UMR 5563, CNRS-OMP-Université Paul Sabatier, 14 Avenue Edouard Belin, 31400 Toulouse, France
[b] CEREGE, CNRS-Université Paul Cézanne Aix Marseille III, BP 80, 13545 Aix-en-Provence, France

Received 8 July 2005; accepted in revised form 22 December 2005

Abstract

Although phytoliths, constituted mainly by micrometric opal, exhibit an important control on silicon cycle in superficial continental environments, their thermodynamic properties and reactivity in aqueous solution are still poorly known. In this work, we determined the solubility and dissolution rates of bamboo phytoliths collected in the Réunion Island and characterized their surface properties via electrophoretic measurements and potentiometric titrations in a wide range of pH. The solubility product of "soil" phytoliths ($pK^0_{sp} = 2.74$ at 25 °C) is equal to that of vitreous silica and is 17 times higher than that of quartz. Similarly, the enthalpy of phytoliths dissolution reaction ($\Delta H_r^{25-80°C} = 10.85$ kJ/mol) is close to that of amorphous silica but is significantly lower than the enthalpy of quartz dissolution. Electrophoretic measurements yield isoelectric point $pH_{IEP} = 1.2 \pm 0.1$ and 2.5 ± 0.2 for "soil" (native) and "heated" (450 °C heating to remove organic matter) phytoliths, respectively. Surface acid–base titrations allowed generation of a 2-pK surface complexation model. Phytoliths dissolution rates, measured in mixed-flow reactors at far from equilibrium conditions at $2 \leqslant pH \leqslant 12$, were found to be intermediate between those of quartz and vitreous silica. The dissolution rate dependence on pH was modeled within the concept of surface coordination theory using the equation:

$$R = k_1 \cdot \{> SiOH_2^+\}^n + k_2 \cdot \{> SiOH^0\} + k_3 \cdot \{> SiO^-\}^m,$$

where $\{>i\}$ stands for the concentration of the surface species present at the SiO_2–H_2O interface, k_i are the rate constants of the three parallel reactions and n and m represent the order of the proton- and hydroxy-promoted reactions, respectively. It follows from the results of this study that phytoliths dissolution rates exhibit a minimum at pH ~ 3. This can explain their good preservation in the acidic soil horizons of Réunion Island. In terms of silicon biogeochemical cycle, phytoliths represent a large buffering reservoir, which can play an important role in the regulation of silica fluxes in terrestrial aquatic environments.

1. Introduction

Silicon is, in the form of tetrahedral SiO_4 groups, a major constituent of silicate minerals (feldspaths, amphiboles, and pyroxenes) which represent more than 75% of the earth surface rocks. Since the pioneering works of Sillén (1961), Mackenzie and Garrels (1966a,b), and Wollast and Mackensie (1983), many studies have been aimed at characterizing the global cycle of silicon, however, it is only recently that the importance of the biogenic cycle of this element in terrestrial environments has been recognized (Meunier et al., 1999; Derry et al., 2005). Indeed, it has been shown that a significant amount of silicic acid, that controls silicon transport in porewaters, can be trapped by plant roots and precipitated in aerial tissues cells as micrometric opal particles called phytoliths. Phytoliths are released during

* Corresponding author. Fax: 33 5 61 33 25 60.
E-mail addresses: fraysse@lmtg.obs-mip.fr (F. Fraysse), oleg@lmtg.obs-mip.fr (O.S. Pokrovsky).

0016-7037/$ - see front matter © 2006 Elsevier Inc. All rights reserved.
doi:10.1016/j.gca.2005.12.025

organic matter degradation in litter horizon and subsequently transferred to deeper horizons or evacuated by aerial or hydrographical ways (Bartoli, 1981; Piperno, 1988). Alexandre et al. (1997) have shown that in Dimonika latosoils (Congo) the contribution of phytoliths to the flux of dissolved silica exported from the weathering profile is three times larger than that issued from non-biogenic silicate minerals dissolution. Derry et al. (2005) demonstrated the importance of plants in controlling the Si flux in Hawaiian streams, and Pokrovsky et al. (2005) estimated that at least 30% of total Si flux exported by Central Siberian rivers could be linked to plant litter degradation. Another illustration of the important contribution of phytoliths to the silicon soil reservoir is given by Meunier et al. (1999, 2001) who described, in the Réunion Island andosoils, a 15-cm thick layer of biogenic silica originated from bamboos forest fires.

These results strongly suggest that silicon recycling by plants could not be ignored during analysis of weathering processes. At the present time, however, quantification of this recycling is difficult due to the lack of data on the surface properties, solubility and reactivity of natural phytoliths. The aim of this work is to acquire this necessary information by applying several complementary physico-chemical techniques to phytoliths collected in a soil horizon of Réunion Island. Thanks to sufficient amount of phytoliths collected from this site, we were able, for the first time, to characterize rigorously their physico-chemical properties and reactivity. In this regard, Réunion phytoliths are unique but they should be representative for all other phytoliths originated from bamboos.

2. Materials and methods

2.1. Phytoliths characterization

Phytoliths are formed by migration and precipitation, in the lap of bamboos, of aqueous silica present in soil porewaters. Generally, after plant litter degradation, the phytoliths are released in the upper soil horizons. The phytoliths investigated in this study originate from a 15-cm thick phytolith rich horizon developed on the west side of the ''Piton des Neiges'' volcano (La Réunion Island) around 745 years ago after intense forest fires (Meunier et al., 1999). They have been sampled at a depth of 20 cm in M horizon of andosoils and are mainly represented by debris of leaves and stems of *Nastus borbonicus* (Meunier et al., 1999). The fresh phytoliths were extracted from contemporary bamboo of the Réunion Island using the dry method (Kelly, 1990) which consists in washing in 1N HCl plant pieces (leaves, stems, and roots) and heating them in an oven at 450 °C during 6 h.

The phytoliths have a size between 2 and 60 μm and are mainly composed of silica (~92 wt%), water (~6 wt%) with some amount of carbon (1.7%), and traces of Al (0.04%) and Fe (0.08%) (Meunier et al., 1999). They were sieved to separate the particles smaller than 50 μm from large plant debris.

Three types of samples were used in this study: ''soil,'' ''heated'' and ''fresh'' phytoliths (Table 1). To prevent the destruction of fine structure, ''soil'' phytoliths were not subjected to any specific treatment after extraction from the soil. These phytoliths were used in most experiments performed in the present study. ''Heated,'' phytoliths were obtained by heating soil phytoliths at 450 °C during 6 h to remove the organic matter by combustion. ''Fresh'' phytoliths were extracted from contemporary bamboo (*N. borbonicus*) (Meunier et al., 1999). The specific surface areas (SSA) of ''soil,'' ''heated'' and ''fresh'' bamboo phytoliths were 5.2 ± 0.1, 6.5 ± 0.1, and $159.5 \pm 0.1\ m^2/g$, respectively, as determined by N_2 multipoint adsorption using the BET method. The main reason for the large differences in SSA of fresh and soil or heated phytoliths is the disappearance of fine structures of samples and thin cell walls covered by silica due to phytoliths aging and partial dissolution during several hundreds years in soil horizon. Besides, the ''fresh'' phytoliths were prepared from ground vegetation samples which could also decrease the particle size as it was confirmed by the SEM observations.

The differential thermal gravimetry (DTG) analysis of ''soil'' phytoliths showed that they exhibited the same weight loss (~6% at 50 °C) than amorphous silica (Baker silicic acid: $SiO_2{\cdot}2.2H_2O$) which corresponds to the removal of non-structural water. ''Soil'' and ''heated'' phytoliths exhibited similar diffuse reflectance infrared Fourier transformed (DRIFT) spectra although the bands of aliphatic carbon groups at 2960, 2925, and 2850 cm^{-1} disappear after thermal treatment. The characteristic bands of SiOH hydroxyls (3350 and 1630 cm^{-1}) and Si–O–Si bands at 1092, 952, and 799 cm^{-1}, also present on amorphous silica,

Table 1
Types of phytoliths used in this study

Type of phytoliths	Origin	Treatment	SSA (m^2/g)	Type of experiments
Soil	Bamboo litter	None	5.18	Solubility, electrophoresis, dissolution kinetics, DTG, DRIFT, XPS, SEM
Heated	Bamboo litter	Heated at 450 °C	6.51	Surface titration, electrophoresis, dissolution kinetics, DTG, DRIFT, XPS
Fresh	Fresh bamboo	1 N HCl washing + heated at 450 °C	159.5	Electrophoresis, dissolution kinetics

SSA, specific surface area.

were detected on both samples. Similar to previous studies (i.e., Koretsky et al., 1997), evidence of H-bonded OH groups was found after heating at 450 °C, although no definitive identification of these groups as geminal >$Si(OH)_2$, vicinal >Si(OH), or residual H_2O/H-bonded surface groups was possible.

In order to characterize the surface composition of phytoliths, X-ray photoelectron spectroscopy (XPS) has been used. XPS is a widespread method for the chemical analysis of solid surfaces (i.e., Pokrovsky and Schott, 2000; Gélabert et al., 2004). Due to the shallow depth of X-ray beam penetration inside the material (up to 10 nm), this technique allows quantitative analysis of phytoliths surface without interference from the inner (bulk) of the solid. "Soil" phytoliths, "heated" phytoliths and ground "heated" phytoliths were analyzed via XPS. In this way, the interior composition of "heated" phytoliths could be contrasted to that of their surface and to "Soil" phytoliths by comparing XPS peak ratios for unground and ground material, respectively. Analyses were conducted on an ESCALAB VG 220i-XL spectrometer. A non-monochromatic twin Mg K_α X-ray radiation was used as the excitation source at a power of 200 W. Analyzing pass energy of 20 eV with a step size of 0.10 eV was used. The reproducibility of measured atomic ratios for phytoliths surfaces was better than 10% allowing to quantitatively measure the surface concentrations of carbon, oxygen, and silicon.

2.2. Solubility measurements

The solubility of "soil" phytoliths was measured at 25, 50, and 80 °C in 0.01 M NaCl solutions, at pH = 4, 6, and 8 obtained by addition of 0.01 M HCl or NaOH solution. Phytoliths suspension of 16 g/L was prepared in 25 mL polypropylene flasks and kept in an air thermostated chamber at 25, 50, and 80 °C. The reaction progress was monitored by measuring dissolved silica concentration as a function of time. Five to six milliliters aliquots of the reacting solution were removed at predetermined times for pH measurement, centrifuged during 10 min at 2500*g* and filtered through 0.22 μm cellulose ester membrane for aqueous silica analysis. The samples were continuously shaken with an automatic shaker. The pH of suspension remained stable within 0.05 U as verified by periodical measurements.

Solution pH was measured using a combination glass electrode (Mettler Toledo) calibrated with NIST buffers (pH 4.01, 6.865, 9.18 at 25 °C). Precision of pH measurements was ±0.01–0.005 U. The pH values at 50 and 80 °C were computed using MINTEQA2 (Allison et al., 1991) from solution composition and pH measured at 25 °C. The uncertainty associated with these calculations achieves 0.05 pH units. pH measurements at 25 °C in highly acidic solutions of elevated ionic strengths (pH < 2) were performed after electrode calibration during titration of nitrogen-saturated 0.1–1.0 M $NaNO_3$ solutions by standardized 0.1–1 M HCl solutions and computing a_{H^+} using the Davis equation which has been shown to be valid to 0.7 M ionic strength (Pokrovsky and Savenko, 1992, 1996). Precision of pH measurement was ±0.02 U at $1 \leqslant pH \leqslant 3$ and ±0.03 U at pH < 1.

Aqueous silica concentration was determined using the molybdate blue method and a Technicon Autoanalyser II with an uncertainty of 2% and a detection limit of 7×10^{-7} M.

2.3. Electrophoretic measurements

Microelectrophoresis, which is a powerful technique for characterization of the electric double layer (EDL) of dispersive particles (see Hunter, 1989; Lyklema et al., 1998; Van der Wal et al., 1997; for principles and discussions), was used to determine the phytoliths zeta potential (ζ) as a function of pH and ionic strength and thus to quantify the pH of the isoelectric point (pH_{IEP}) when ζ is equal to zero.

Phytoliths electrophoretic mobilities were determined using a microelectrophoremeter ("Zetaphoremeter IV" Z 4000, CAD Instrumentation) following the technique described elsewhere (Gélabert et al., 2004; Pokrovsky and Schott, 2004).

The electrophoretic mobility of the particles was converted into zeta potential using the Smoluchowski–Helmholtz equation.

$$\zeta = \frac{(\varepsilon \times \mu_E)}{(4\pi \times \eta)}, \quad (1)$$

where ζ stands for the zeta potential (mV) and ε, η, and μ_E represent the dielectric constant of the solution, the viscosity and the electrophoretic mobility, respectively. Because of its simplicity, Smoluchowski's equation is widely used for calculating zeta potentials from the electrophoretic mobilities of quartz (Li and De Bruyn, 1966; Kosmulski et al., 2002), silicas (Xu et al., 2003; Gun'ko et al., 2005), carbonates (Pokrovsky et al., 1999) and biological materials (Van der Wal et al., 1997; Wilson et al., 2001). Note that the use of more sophisticated equations for calculating zeta potentials of natural phytoliths suspension is not feasible due to (i) the absence of information on surface conductance and (ii) irregular shape of bamboo's phytoliths debris precluding to use the theory of electrokinetic migration of spherical particles.

Experiments were performed in solutions of ionic strength and pH ranging from 0.001 to 0.05 M (NaCl, HCl, and NaOH) and 1.5–11, respectively. Typically, three replicates were carried out at each pH value providing an uncertainty of ±10%.

2.4. Surface titration

Acid–base surface titrations, aimed at determination of phytoliths surface electric charge as a function of pH, were performed using a DL70ES Mettler Toledo automatic titrator equipped with a high resolution (0.1 mV) pH-meter. Experiments were performed at 25 °C with "heated"

phytoliths, vitreous silica (Prolabo) and silicic acid $SiO_2{\cdot}2.2H_2O$ (Baker) having surface areas of 6.5, 4.85, and 462 m^2/g, respectively. Prior the titration, solid suspensions were let equilibrate with the electrolyte solution for 2 h. Standardized 0.02 M NaOH and 0.01 M HCl solutions were used for titration of background electrolytes (0.01, 0.05, and 0.5 M NaCl) and 20 g/L phytoliths suspensions in 0.01, 0.05, and 0.5 M NaCl. The suspensions were continuously stirred and purged with N_2 gas. After electrode calibration, the solutions were acidified to $pH = 4 \pm 0.2$ by adding known amount of HCl, and titration started with automatic injection of 5–50 μL of volume of NaOH with a pH step of 0.1–12 mV. For each titration point, the pH was recorded once the steady state conditions were achieved (potential drift < 0.5 mV/min).

The excess surface proton concentration $[H^+]_s$ at each pH_j titration point (j) was calculated as

$$[H^+]_s = (C_{aj}(\text{suspension}) - C_{aj}(\text{electrolyte})) - (C_{bj}(\text{suspension}) - C_{bj}(\text{electrolyte})), \quad (2)$$

where C_{aj} and C_{bj} correspond to the concentrations of acid and base (mol/L) for the jth addition of titrant to phytoliths suspension or background electrolyte at the same pH_j.

The surface charge (Q) is defined as

$$Q = \frac{[H^+]_s}{m \times S}, \quad (3)$$

where m is the mass concentration of phytoliths in solution (g/L) and S is their specific surface area (m^2/g). Release of silica in solution during the titration of amorphous SiO_2 is known to affect strongly the surface charge determination via potentiometric titration at alkaline pHs (i.e., Goyne et al., 2002). Regular measurements of [Si] in phytoliths suspension subjected to titration at pH above 7 allowed to account for the effect of bulk solid dissolution and hydroxyl ions consumption; these corrections never exceeded 10% of total amount of adsorbed OH^- ions.

2.5. Dissolution kinetics

Phytoliths dissolution rates were measured in continuously stirred mixed flow reactors having ~30 mL volume (Fig. 1) and plunged in a thermostated water-bath at 25 ± 0.5 °C. In each reactor, from 0.2 to 0.5 g phytoliths were kept suspended using a Teflon coated suspended stirbar driven by a magnetic stir plate located beneath the reactor. The solution left the reactor through a 2.5-μm pore size polypropylene filter (Millipore) mounted on a 47-mm diameter polypropylene filter holder. Solutions were injected in the reactor by a peristaltic pump allowing adjusting the flow rate between 0.1 and 1 mL/min. Reacting solutions were prepared at an ionic strength of 0.01 M (NaCl, NaOH, and HCl) and pH ranging from 2 to 12. At pH < 2, a constant ionic strength of 0.1 M (NaCl + HCl) was maintained.

The rate of phytoliths dissolution (R, mol/cm^2/s) was calculated as

$$R = \frac{(C_{out} - C_{in}) \times Q}{m \times S}, \quad (4)$$

where C_{out} and C_{in} represent silica concentration in output and input fluids (mol/L), respectively, Q is the flow rate (L/s), m is the mass of phytoliths in the reactor (g) and S is the initial specific area of phytoliths (cm^2/g). The evolution of phytoliths BET specific surface area (SSA) in the course of dissolution has been monitored at $pH = 7.5 \pm 0.2$. Unlike quartz SSA that increases with the mass of quartz dissolved (Gautier et al., 2001), phytoliths SSA decreases by about 30% after 1 month reaction corresponding to dissolution of 30% of initial mass. Such a decrease in specific surface area is likely related to the preferential dissolution of fine particles adhering to phytolith surface or microstructure heterogeneities.

3. Results and discussion

3.1. Phytoliths solubility

Aqueous silica concentrations measured as a function of time exposure at 25, 50, and 80 °C and pH = 4, 6, and 8 (measured at 25 °C) are listed in Table A1 of Appendix A. The evolution as a function of time of aqueous silica concentration at 25 and 50 °C for the three investigated pH values is reported in Figs. 2A and B. It can be seen that

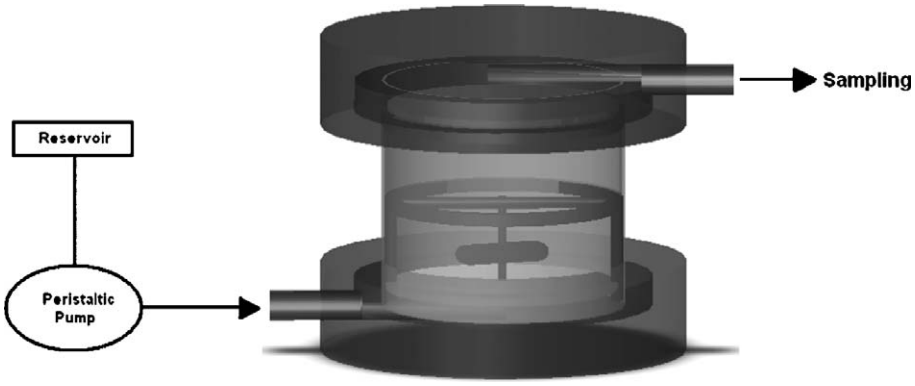

Fig. 1. Schema of a flow through reactor used in experiments.

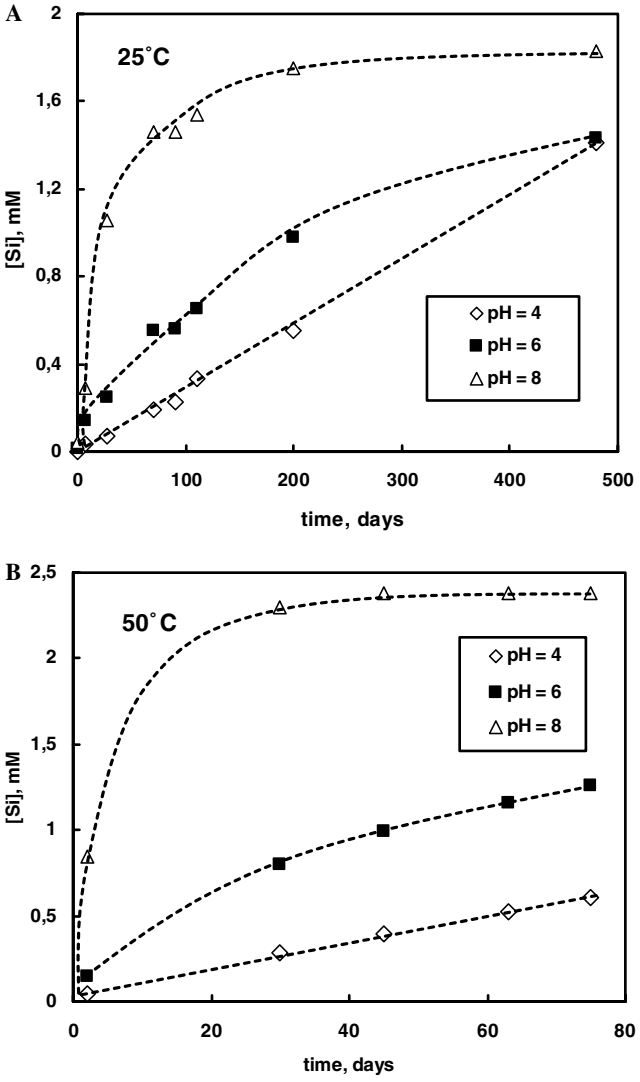

Fig. 2. Batch silica concentration of soil phytoliths as a function of reaction time at pH = 4, 6, and 8, $I = 0.01$ M, at 25 °C (A) and 50 °C (B). The symbols represent the experimental data and the dashed connecting lines help to visualize the dissolution trend.

phytoliths dissolution rate and consequently the approach of equilibrium depend both on temperature and solutions pH. At pH 4 and 6, attainment of steady-state silicic acid concentrations was not reached even after 480, 75, and 40 days at 25, 50, and 80 °C, respectively. Steady-state Si concentration was only reached at pH 8 and equals 0.00183, 0.00238, and 0.0036 M at 25, 50, and 80 °C, respectively. Assuming that these values correspond to the equilibrium between the phytoliths and aqueous solution, it was possible to calculate phytoliths solubility product (K°_{sp}) from

$$SiO_{2(s)} + 2H_2O = H_4SiO^{\circ}_{4(aq)}, \quad K^{\circ}_{(aq)} \tag{5}$$

taking into account silicic acid first hydrolysis (concentration of $H_2SiO_4^{2-}$ represented less than 1% total aqueous silica at our experimental conditions)

$$H_4SiO^{\circ}_{4(aq)} = H_3SiO^{-}_{4\,(aq)} + H^{+}, \quad K_1 \tag{6}$$

and aqueous silica mass balance

$$[SiO_{2(aq)}]_{tot} = [H_4SiO^{\circ}_{4(aq)}] + [H_3SiO^{-}_{4\,(aq)}] \tag{7}$$

where $[i]$ stands for the molality of species i.

Combination of Eqs. (1)–(3) yields the following expression for K°_{sp}:

$$K^{\circ}_{sp} = a_{H_4SiO^{\circ}_4} = [H_4SiO^{\circ}_{4(aq)}] = \frac{\lfloor SiO_{2(aq)} \rfloor}{\left(1 + \frac{K_1}{\gamma_{H_3SiO_4^-} \times a_{H^+}}\right)}, \tag{8}$$

where K_1 is taken from Busey and Mesmer (1977) ($K_{1,25\,^{\circ}C} = 10^{-9.82}$; $K_{1,50\,^{\circ}C} = 10^{-9.51}$; and $K_{1,80\,^{\circ}C} = 10^{-9.23}$) and $\gamma H_3SiO_4^-$ the activity coefficient of $H_3SiO_4^-$ is calculated using the Davies equation (Allison et al., 1991). Note that the uncertainty associated with pH calculations at 50 and 80 °C (0.05 pH units, see Section 2.2) do not affect the calculation of K°_{sp} at pH ~ 8 using Eq. (8) as $K_{1,80\,^{\circ}C} = 10^{-9.23}$. Values of the logarithm of phytoliths solubility product derived in this study are listed in Table 2. These values, together with corresponding values for quartz and amorphous silica (Rimstidt and Barnes, 1980), are plotted as a function of reciprocal temperature in Fig. 3. It can be seen that the solubility product of phytoliths is slightly lower than that of amorphous silica but ~10 times higher than that of quartz. The enthalpy of phytoliths dissolution derived in this study from the Van't Hoff equation

$$\frac{\partial \ln K}{\partial T} = \frac{\Delta H_r}{RT^2} \tag{9}$$

($\Delta H_r^{25-80^{\circ}C} = 10.85$ kJ/mol) is comparable with corresponding value for amorphous silica (14.44 kJ/mol; Rimstidt and Barnes, 1980) but is significantly lower than the enthalpy of quartz dissolution (25.63 kJ/mol; Rimstidt and Barnes, 1980). These differences between both the Gibbs free energy and enthalpy of dissociation of quartz and amorphous silica and phytoliths are likely to originate from a wider range of ⟨Si–O–Si⟩ bond angles in phytoliths and amorphous silica rather than changes in Si–O distance as reflected by ^{29}Si MAS-NMR spectroscopy of these phases (Navrotsky, 1994; Schott et al., 2002).

3.2. Electrophoretic measurements

Results of electrophoretic measurements are listed in Table A2 of Appendix B and illustrated in Figs. 4A and B that represent phytoliths zeta potential (ζ), determined in 0.001, 0.01, and 0.05 mol/L HCl/NaCl/NaOH solutions,

Table 2
Soil phytoliths solubility

Temperature (°C)	C_{SiO_2} mmol/L	$\log K^{\circ}_{sp}$ phytoliths
25	1.83	−2.74
50	2.38	−2.62
80	3.6	−2.44

Silica concentrations at steady state and pH = 8.00 ± 0.05 and $\log K^{\circ}_{sp}$, as a function of temperature.

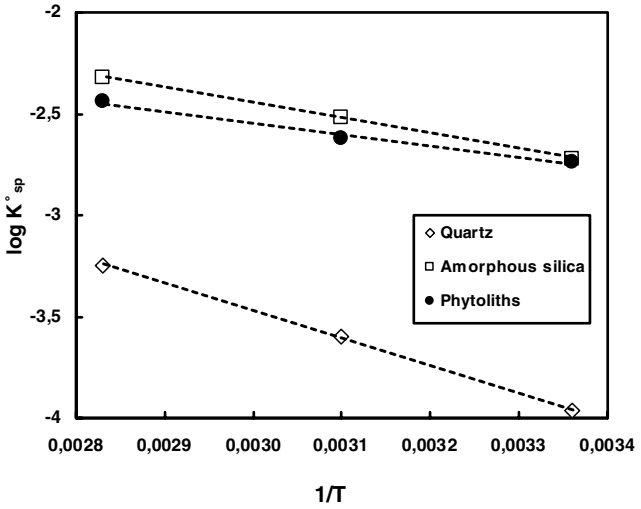

Fig. 3. Log K°_{sp} of soil phytoliths (this study), quartz and amorphous silica (Rimstidt and Barnes, 1980) as a function of the inverse of temperature. The symbols represent the experimental data and dashed lines are the linear fit by Van't Hoff equation Eq. (9).

as a function of pH at 25 °C. Phytoliths exhibit a negative zeta potential at pH > 1.5 which reflects their surface bearing a negative charge. Like for the other silica phases, ζ absolute value increases with increasing pH and ionic strength. The pH of isoelectric point (pH_{IEP}) was determined by linear extrapolation of ζ–pH plots obtained at different ionic strengths to zero zeta potential; in this regard, the pH_{IEP} can be considered as common intersection point. The pH_{IEP} of "soil" phytoliths is 1.2 ± 0.1 which is comparable to that of quartz ($pH_{IEP} = 1.5$–3) but lower than that of amorphous silica ($pH_{IEP} = 2$–4). The pH_{IEP} of "heated" phytoliths (i.e., organic matter-free) is higher ($pH_{IEP} = 2.5 \pm 0.2$, Fig. 4B). This difference can be explained by the interaction of neutral and negatively charged organic moieties with $>SiOH_2^+$ surface groups that prevents the latters to contribute to positive surface potential. Indeed, the XPS analysis of different phytoliths revealed strong enrichment of "soil" phytoliths surface in organic carbon compared to heated and grinded phytoliths (Table A3 of the Appendix C).

The only work available on phytoliths' electrophoretic properties is that of Bartoli (1985) who reported a $pH_{IEP} \sim 5$ for phytoliths from conifers and beeches. However, his phytoliths contained more aluminum than those investigated in the present study (8 versus 0.14 Al_2O_3 weight %) and are likely to be contaminated by Al oxides/hydroxides. Because the pH of isoelectric point for aluminum oxides (~8.5–9) is much higher than that of SiO_2, it is possible that the aluminol surface groups ($>AlOH_2^+$) in phytoliths of Bartoli (1985) provide an overall positive charge in the acid pH region.

3.3. Surface titration and surface complexation model

Results of surface potentiometric titrations are illustrated in Fig. 5 and reported in Table A3 of Appendix C. The

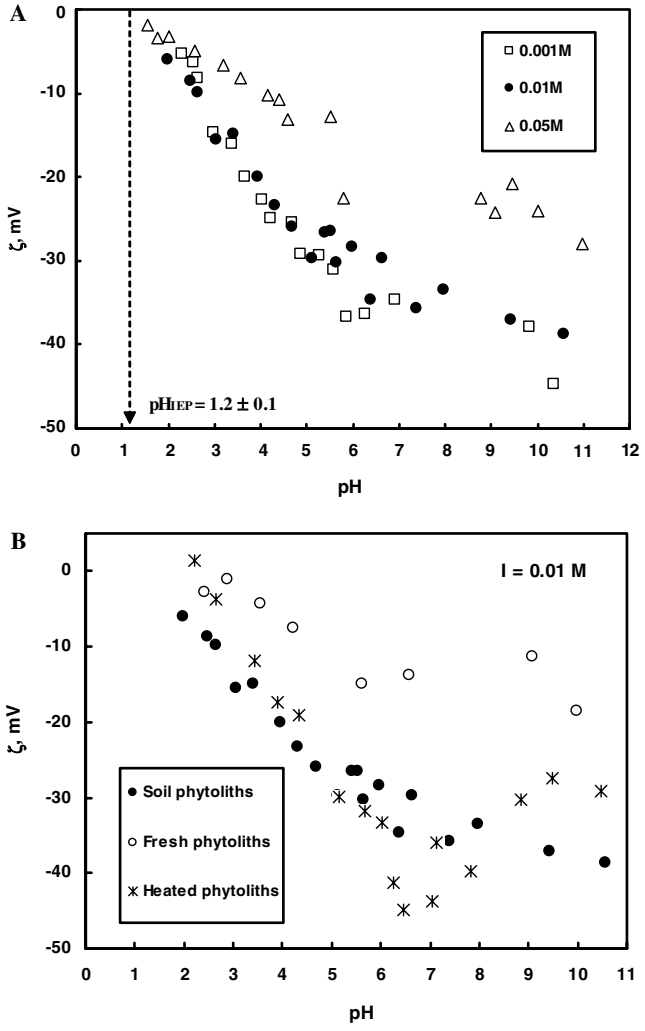

Fig. 4. (A) Zeta potential of soil phytoliths measured at 25 °C as a function of pH and ionic strengths. (B) Zeta potential of soil, heated and fresh phytoliths measured at 25 °C as a function of pH and constant ionic strength of 0.01 M.

surface charge is negative at pH > 4.5 like it is the case for other silicon oxides (Stumm, 1992) and it increases with the increase of the ionic strength (I). These results have been fitted using FITEQL program (Herbelin and Westall, 1996) for $I = 0.01$, 0.05, and 0.5 M, assuming the constant capacitance of the electric double layer (CCM) and a density of surface silanol groups of 16 μmol/m^2, a value often used in surface complexation modeling (e.g., Sverjensky and Sahai, 1996).

Accurate simulation of phytoliths surface charge required values of the capacitance C of the electric double layer of 3, 13, and 35 F/m^2 for I equal to 0.01, 0.05, and 0.5 M, respectively ($C = I^{1/2}/\alpha$ with $\alpha = 0.025 \pm 0.05$), that are significantly higher than those commonly adopted for silica-solution interfaces (i.e., $C = 0.4$–1.7 F/m^2 for $I = 0.7$ M, Dixit and Van Cappellen, 2002). The high value required for the EDL capacitance results from the very high surface charge built up found in this study on phytoliths surfaces. Artifacts of our experimental titrations

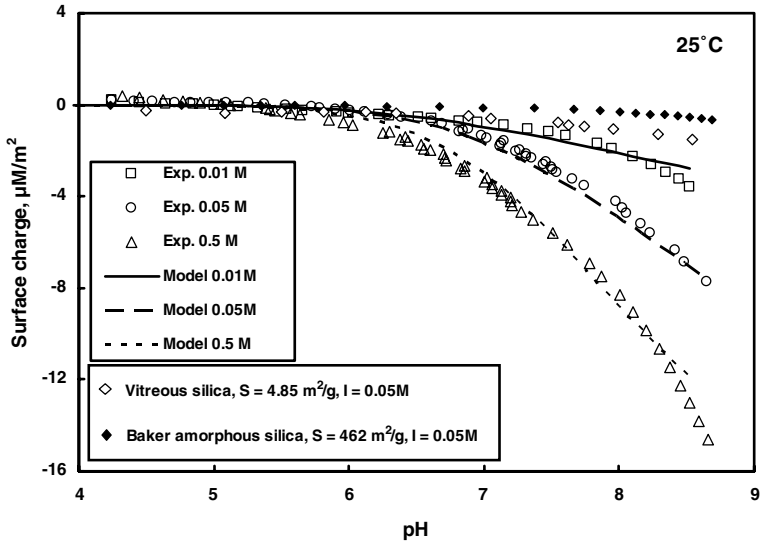

Fig. 5. The surface charge density of heated phytoliths (20 g/L) as a function of pH measured at 25 °C and various ionic strengths: 0.01 M (squares), 0.05 M (circles) and 0.5 M (triangles). The curves were generated from the surface complexation model developed in this study. They are compared to surface charge density of two types of silica measured as a function of pH at $I = 0.05$ M and 25 °C: Baker amorphous silica (5.2 g/L, solid diamonds) and vitreous silica (20 g/L, open diamonds).

procedure cannot explain this high surface charge because additional potentiometric titrations we performed on vitreous silica (SSA = 4.85 m^2/g) and silicic acid (SSA = 462 m^2/g) did not reveal "unusual" OH^- adsorption (Fig. 5) and could be fitted with usual values of the EDL capacitance ($C \sim 0.4$–1.3 F/m^2 for $I = 0.05$ M).

This high surface charge is not related to the surface contamination of heated phytoliths by XPS-detectable organic or inorganic substances as the analyses of "intact" and finely ground "heated" phytoliths did not demonstrate any differences in elementary chemical composition of first 100 Å of the surface (Table A4 of Appendix D). Note also that one cannot invoke a higher surface sites density to account for such a high surface charge as the sites density selected in this study (16 μmol/m^2) corresponds to the maximal value for a monolayer surface coverage and there is no reason to assume that the adsorption of OH^- occurs within multiple surface layers of the biogenic opal. Thus, there is not straightforward explanation for phytoliths high surface charge found in this study, but the presence of trace amounts of surface groups accommodating hydroxyl ions at alkaline pH and/or the development of an OH^- permeable surface layer not accurately quantified by BET surface measurements can not be excluded. In this regard, note that Hiemstra et al. (1996) show that on silica surfaces, singly coordinated groups are present in isolated pairs, protruding the surface and thus creating a layer penetrable for water molecules. He further argued that this type of surface structure is responsible for the relative high stern layer capacitance.

The best fit to the experimental data was achieved with $\log K_{10} = -7.67 \pm 0.1$, -7.73 ± 0.1, and -7.50 ± 0.1 for $I = 0.01$, 0.05, and 0.5 M, respectively, for the deprotonation reaction

$$> SiOH^\circ - H^+ => SiO^-, \quad K_{10} \tag{10}$$

The stability constant of silanol group protonation reaction

$$> SiOH^\circ + H^+ => SiOH_2^+, \quad K_{11} \tag{11}$$

could be assessed from the pH_{IEP} of "heated" phytoliths (Section 2.5) using the relationship

$$pH_{IEP} = (pK_{10} - pK_{11})/2 \tag{12}$$

that gives $pK_{11} = 2.67 \pm 0.1$ for $I = 0.01$ M.

It can be seen from Fig. 5 that a reasonable agreement between the model and the experimental data is observed for the three ionic strengths investigated.

3.4. Dissolution kinetics and behavior of phytoliths in natural settings

Scanning electron microphotographs of "soil" phytoliths obtained before and after dissolution experiments, during 1 month at pH 7.5 ± 0.2 are presented in Figs. 6A–C, respectively). No major change in morphology of grains was observed but the disappearance of fine particles adhering to surface of initial grains is worth nothing. The last observation is in accord with SSA decrease from 5.18 to 3.58 m^2/g (Section 2.5). "Fresh" phytoliths exhibit fine structures of samples and thin cell walls covered by silica (Fig. 6D) consistent with their much higher surface area.

Mechanical steady-state conditions (corresponding to five times renewing of solution in the reactor as indicated by vertical dashed lines in Fig. 7) were achieved after 8 h to 3 days depending on the flow rate. Examples of chemical steady-state attainment are presented in Fig. 7 where the outlet Si concentration is plotted as a function of time for different pH and flow rates. It can be seen that at

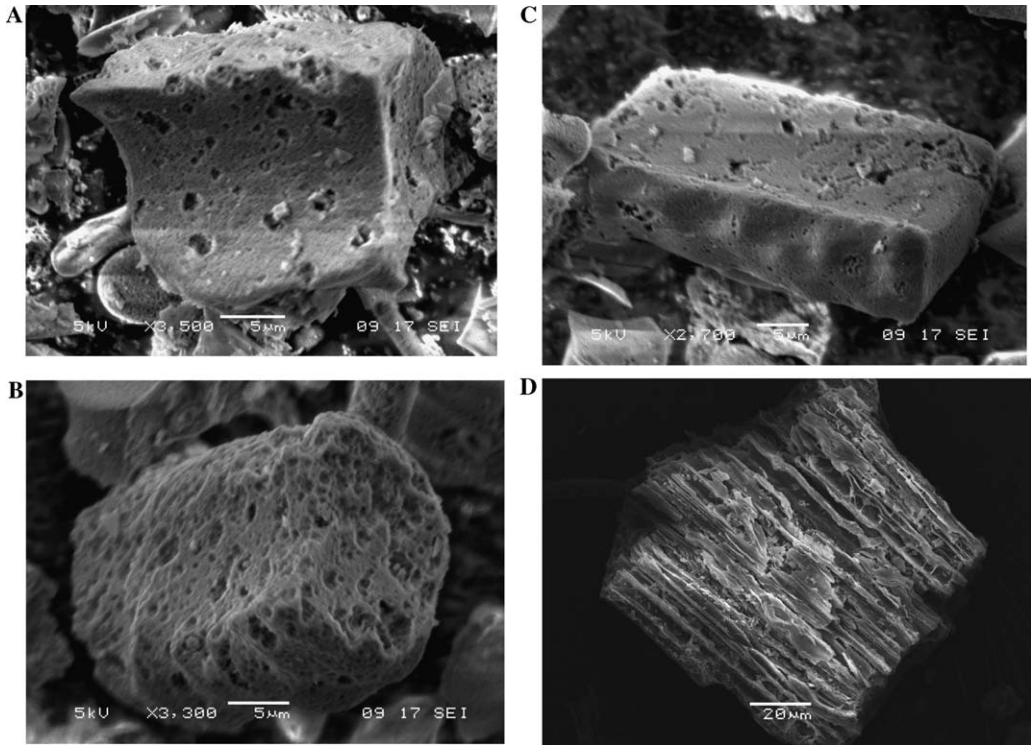

Fig. 6. (A) SEM photomicrograph of soil phytoliths before dissolution in mixed-flow reactor at 25 °C, $S = 5.18$ m^2/g. (B and C) SEM photomicrograph of soil phytoliths after 1 month of dissolution in mixed-flow reactor at 25 °C and pH = 7.5 ± 0.2, $S = 3.58$ m^2/g. The overall massive shape of soil phytoliths remains unchanged and no new pores and pit holes were formed. (D) SEM photomicrograph of fresh phytoliths after 18 days at pH 2.

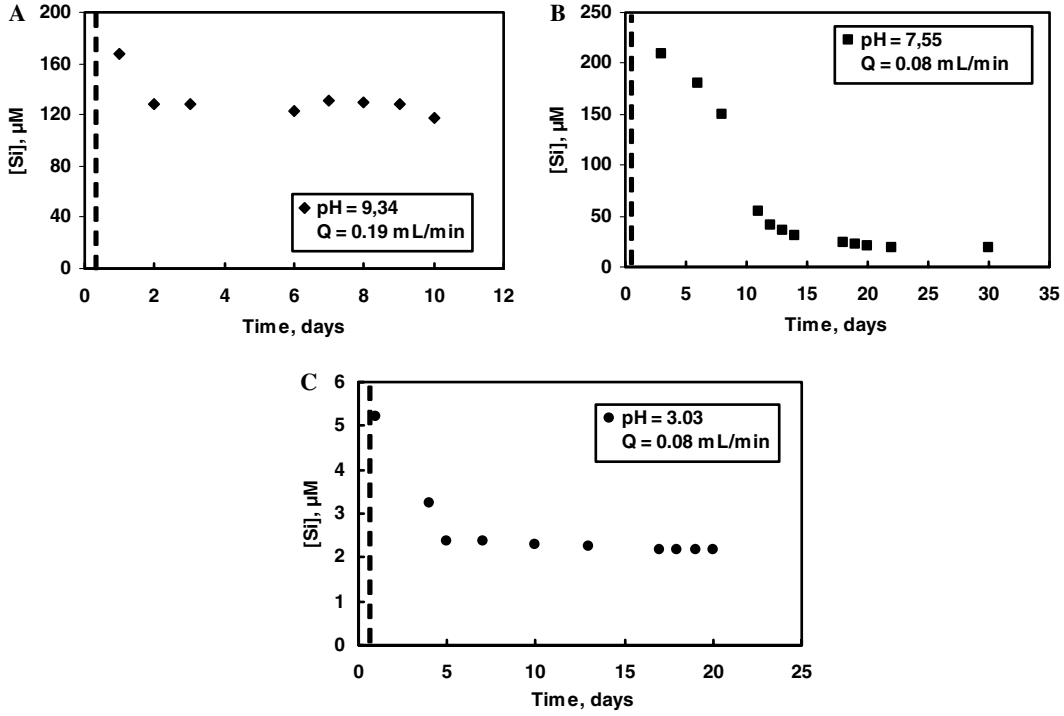

Fig. 7. Examples of steady state attainment for outlet Si concentration in the mixed-flow reactor as a function of time and pH of 9.34 (A), 7.55 (B), and 3.03 (C). The symbols represent the experimental data and the dashed line defines the mechanical steady state in reactor.

pH = 3.03, 7.55, and 9.34, after 15, 25, and 6 days (corresponding to 77, 115, and 90 reactor volumes of input solution passed through the reactor), respectively, outlet Si concentration remains constant within ±10% which was considered as the steady-state concentration used to calculate dissolution rates.

Values of steady state dissolution rates obtained at ionic strength from 0.01 M (NaCl, NaOH, and HCl) to 0.1 M for all types of phytoliths are listed in Table 3 and plotted as a function of pH in Fig. 8. For comparison, corresponding results reported for quartz and vitreous silica by Dove and Elston (1992) and Wirth and Gieskes (1979), respectively, are shown in this figure. No significant differences in the BET surface-normalized dissolution rates of all three types of phytoliths were detected.

It can be seen that the rate data define three pH regions. In strongly acidic solutions (pH < 2), rates increase with a_{H^+}. At $2 \leqslant pH \leqslant 3$–4, the rates are independent on pH and exhibit a minimal value of 5×10^{-17} mol/cm^2/s. At pH from 4 to 12, rates increase with pH with a slope of 0.33 very close to that measured for quartz and amorphous silica.

Table 3
Dissolution rates R of bamboo phytoliths in mixed-flow reactor at 25 °C

Exp. No.	Flow (ml/min)	[Si] (μmol/L)	pH	R (mol/cm^2/s)
Soil phytoliths, $S_{initial}$ = 5.18 m^2/g; S_{final} = 3.58 m^2/g at pH = 7.5 ± 0.2, m = 0.5 g				
1–26	0.076	10.10	1.00 ± 0.1	1.65E−16
1–27	0.076	3.29	1.32	5.36E−17
1–25	0.083	2.93	2.00 ± 0.1	5.22E−17
1–24	0.084	3.21	2.97	5.78E−17
1–23	0.078	8.76	4.17	1.47E−16
1–8	0.22	1.71	4.94	2.42E−16
1–11	0.21	2.07	5.07	2.80E−16
1–1	0.22	2.22	5.10 ± 0.1	3.14E−16
1–12	0.21	2.04	5.19	2.76E−16
1–13	0.21	2.32	5.31	3.14E−16
2–1	0.22	2.82	5.32	3.99E−16
2–25	0.087	5.79	5.40 ± 0.1	3.24E−16
2–26	0.086	6.43	5.54	3.56E−16
2–27	0.087	7.08	5.81	3.96E−16
2–22	0.088	10.20	5.89	5.78E−16
1–22	0.06	105.00	6.73	1.35E−15
2–31	0.078	18.90	7.55	9.49E−16
1–31	0.08	45.10	8.00 ± 0.1	2.32E−15
2–32	0.198	70.0	8.78	8.92E−15
2–17	0.214	321.00	10.04	4.42E−14
2–19	0.215	312.00	10.54	4.32E−14
2–7	0.22	487.00	10.62	6.89E−14
2–6–2	0.08	1980.00	11.47	1.02E−13
2–5	0.21	1040.00	11.61	1.41E−13
2–18–2,3	0.08	1320.00	11.62	6.80E−14
2–6–1	0.20	1150.00	11.80 ± 0.1	1.48E−13
2–18–1	0.20	841.00	11.85	1.08E−13
Heated phytoliths, S = 6.51 m^2/g, m = 1 g				
3–26	0.059	20.10	1.02	2.94E−16
3–27	0.069	6.45	1.32	1.10E−16
3–25	0.064	8.00	2.00 ± 0.1	1.10E−16
3–24	0.083	8.57	3.00 ± 0.1	1.76E−16
3–21	0.58	372.00	11.28	5.35E−14
Fresh phytoliths, $S_{initial}$ = 159.5 m^2/g and S_{final} = 73.93 m^2/g (after dissolution). m = 0.1 g for 2–36 and 3–32; m = 0.05 g for 1–36				
2–36	0.081	2.17	3.02	1.76E−16
1–36	0.052	42.66	6.36	1.10E−16
3–32	0.196	53.00	7.00 ± 0.1	2.33E−15

0.05 M ⩽ I ⩽ 0.1 M for pH < 2 and $I = 0.01$ M for pH > 2. Uncertainty on pH values are ±0.05 U unless indicated.

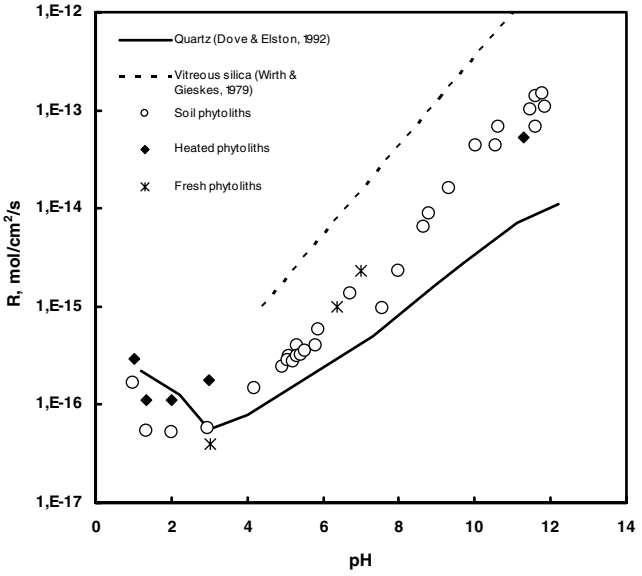

Fig. 8. Dissolution rates of soil, heated and fresh phytoliths as a function of pH measured in mixed-flow reactor at 25 °C, $I = 0.01$ M for $2 \leqslant pH \leqslant 12$ and $I = 0.1$ M for pH < 2. Symbols, experimental data; solid line, rates of quartz (Dove and Elston, 1992); dashed line, rates of vitreous silica (Wirth and Gieskes, 1979). Uncertainties of rate measurements are within the size of symbols.

Phytoliths dissolution rates can be modeled within the framework of the surface complexation approach (Stumm, 1992) assuming the rate is controlled by the protonation, deprotonation, and hydrolysis of surface >SiOH groups according to (Guy and Schott, 1989; Brady and Walther, 1990; Hiemstra and Van Riemsdijk, 1990; Schott, 1990; Dove, 1996; Duval et al., 2002)

$$R = k_1 \cdot \{> SiOH_2^+\}^n + k_2 \cdot \{> SiOH^0\} + k_3 \cdot \{> SiO^-\}^m, \quad (13)$$

where $\{>i\}$ stands for the concentration of the surface species present at the SiO_2–H_2O interface, k_i are the rate constants of the three parallel reactions and n and m represent the order of the proton- and hydroxyl-promoted dissolution reaction, respectively.

At pH > 6, a linear correlation ($r^2 = 0.95$) is observed between log R and log{>SiO$^-$} consistent with $m \sim 2.0$ (Fig. 9). This suggests that the dissolution mechanism requires two preceding deprotonation steps of SiOH groups at the phytoliths surface, in agreement with previous results on quartz (Knauss and Wolery, 1988) and amorphous silica (Wirth and Gieskes, 1979).

Assuming the order of the protonation reaction equals to 1 like it is the case for quartz and vitreous silica (Duval et al., 2002; Pokrovsky et al., 2006), Eq. (13) can be used to fit our rate data in the full pH range. This fitting was performed using non-linear equation by trials and error. The dissolution rate modeling was performed with the surface complexation model (SCM) derived from our surface titration results; for this, the rate data sets of "fresh," "heated," and "soil" phytoliths were compiled together for the fitting

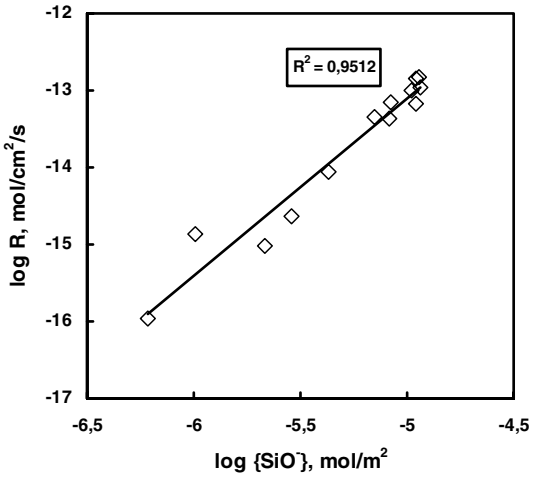

Fig. 9. Correlation between $\log R$ and $\log \{SiO^-\}$ for phytoliths dissolution rates at 25 °C and $6 \leqslant pH \leqslant 12$. Symbols represent experimental data and the line is a linear fit.

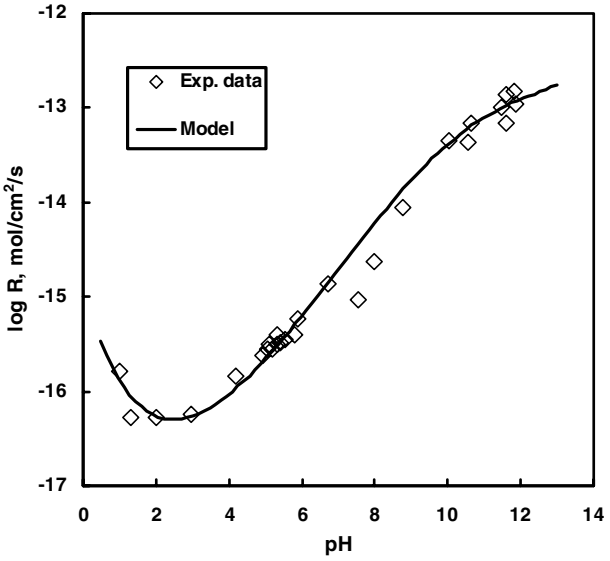

Fig. 10. Modeling of experimental phytoliths dissolution rates at 25 °C and $1 \leqslant pH \leqslant 12$. Symbols represent experimental data and the curve is the SCM fit using Eq. (13).

procedure, assuming the same dissolution mechanism for the three types of phytoliths. The uncertainties attached to parameters of Eq. (13) represent the range of best fit to the rate data, defined as the sum of differences between measured and calculated points. Rates calculated using Eq. (13) are described by the solid line in Fig. 10. They yield

$$k_1 = (2.0 \pm 0.2) \times 10^{-8}\ s^{-1}, \quad n = 1.00 \pm 0.01,$$

$$k_2 = (3.13 \pm 0.3) \times 10^{-12}\ s^{-1},$$

$$k_3 = 0.03 \pm 0.01\ m^2\ mol^{-1}\ s^{-1}, \quad m = 2.0 \pm 0.2$$

for $\{>i\}$ and R expressed in mol/m^2 and $mol/cm^2/s$, respectively Eq. (13).

Because dissolution rates are proportional to the BET surface, and the BET surface-normalized dissolution rates of "soil" and "fresh" phytoliths are similar, one can suggest that, when dissolution rates are mass-normalized rather than surface-normalized, the "fresh" phytoliths are about a factor 30 more reactive than the old "soil" phytoliths. This, again, illustrates the high importance of freshly produced phytoliths in the continental cycle of silica. With their extremely high surface area, these phytoliths represent an easily mobilized pool of silica in soil surface horizons. However, for quantitative assessment of silicon fluxes in vegetal areas, the limiting factor is likely to be the characterization of release of silica from plant litter, where phytoliths are tightly associated with organic matter.

Overall, the SCM-treatment of phytoliths dissolution kinetics indicates that the major rate-controlling mechanisms for different silicon dioxide polymorphs (bamboo phytoliths, quartz, and amorphous silica) are similar. Different phytoliths, depending on their chemical composition with respect to trace elements, are likely to exhibit different surface properties (Bartoli, 1985) and, consequently, reactivities in aqueous solutions. In this regard, comparative study of different origins phytoliths representing terrestrial plants and trees are very timely to better constrain the biogeochemical cycle of silica on land.

4. Conclusions

In this study, several complementary techniques have been used to characterize the surface properties, solubility product and dissolution kinetics of bamboos phytoliths collected in the Réunion Island. Results obtained show that the phytoliths solubility is close to that of amorphous silica while their dissolution rates lay between those of quartz and vitreous silica and exhibit similar pH dependence. Based on electrophoretic measurements and surface titration, a surface complexation model was generated which suggests, in accord with data on quartz (Dove and Elston, 1992; Duval et al., 2002) and amorphous silica (Stumm, 1992; Dixit and Van Cappellen, 2002), the existence of $>SiOH_2^+$, $>SiOH°$, and $>SiO^-$ surface species. At $pH > 6$, dissolution rate is proportional to $\{>SiO^-\}^2$, suggesting that the dissolution mechanism requires two preceding deprotonation steps. It follows from the results of this study that phytoliths dissolution rate reaches a minimum at $pH \sim 3$. This pH value is close to that measured in interstitial solutions of acidic soil horizon of Réunion Island. This explains the good preservation of phytoliths in subsurface soils of this region. Because phytoliths represent important reservoir of biogenic silica in acid soils of tropical and subtropical regions, a comparative study of the reactivity in aqueous solution of (i) phytoliths having various origin and trace metal content and (ii) phytoliths-bearing plant litter debris should allow quantitative modeling of the biogeochemical cycle of terrestrial silicon.

Acknowledgments

We are grateful to D.A. Sverjensky and three anonymous reviewers whose insightful and thorough reviews greatly improve the manuscript. This work was partially supported by the French National Program for Basic Research (ANR "ECCO" project ECOSPHERE CONTINENTALE: Processus et Modélisation). A. Castillo and Th. Aigouy are thanked for careful technical assistance with BET specific surface area measurements and SEM observations, respectively.

Associate editor: Dimitri A. Sverjensky

Appendix A

See Table A1

Appendix B

See Table A2

Appendix C

See Table A3

Table A1
Soil phytoliths solubility

Exposure time (days)	0.1	7	28	70	90	111	200	480
T = 25 °C								
[Si], M pH = 4	1.79E−06	3.64E−05	7.07E−05	1.94E−04	2.29E−04	3.36E−04	5.54E−04	1.41E−03
[Si], M pH = 6	1.41E−05	1.41E−04	2.50E−04	5.50E−04	5.57E−04	6.50E−04	9.82E−04	1.41E−03
[Si], M pH = 8	3.93E−05	2.93E−04	1.06E−03	1.46E−03	1.46E−03	1.54E−03	1.75E−03	1.83E−03
Exposure time (days)	2	30	45	63	75			
T = 50 °C								
[Si], M pH = 4	4.18E−05	2.85E−04	3.93E−04	5.23E−04	6.08E−04			
[Si], M pH = 6	1.50E−04	8.00E−04	9.94E−04	1.16E−03	1.26E−03			
[Si], M pH = 8	8.50E−04	2.30E−03	2.38E−03	2.38E−03	2.38E−03			
Exposure time (days)	6	15	40					
T = 80 °C								
[Si], M pH = 4	1.24E−03	2.80E−03	3.12E−03					
[Si], M pH = 8	2.03E−03	3.40E−03	3.60E−03					

Silical concentration as a function of time.

Table A2
Phytoliths zeta potential (mV) as a function of pH at 25 °C

Soil phytoliths						Heated phytoliths: $I = 0.01$ M		Fresh phytoliths: $I = 0.01$ M	
$I = 0.001$ M		$I = 0.05$ M		$I = 0.01$ M					
pH	ζ (mV)	pH	ζ (mV)	pH	ζ (mV)	pH	ζ (mV)	pH	ζ (mV)
5.57	−31.1 ± 3.1	5.51	−12.8 ± 4.7	5.64	−30.2 ± 4.6	5.67	−31.8 ± 1.9	5.62	−14.8 ± 2.7
5.28	−29.4 ± 4.2	4.6	−13.1 ± 2.0	5.4	−26.6 ± 5.3	5.16	−30.0 ± 4.2	4.21	−7.5 ± 1.1
4.88	−29.2 ± 5.3	4.41	−10.7 ± 1.2	5.12	−29.6 ± 1.6	3.5	−19.1 ± 0.5	3.55	−4.2 ± 1.5
4.68	−25.4 ± 1.9	4.17	−10.2 ± 2.4	4.68	−25.9 ± 0.7	3.91	−17.3 ± 1.4	2.89	−1.0 ± 0.5
4.21	−24.9 ± 0.5	3.57	−8.2± 1.4	8.2	−23.3 ± 1.6	3.43	−11.8 ± 0.5	2.42	−2.8 ± 5.1
4.02	−22.7 ± 1.9	3.20	−6.7 ± 1.6	3.95	−20.0 ± 1.5	2.66	−3.8 ± 1.5	9.97	−18.4 ± 4.1
3.65	−20.1 ± 3.9	2.58	−5.0 ± 2.3	3.40	−14.9 ± 4.3	2.22	+1.5 ± 2.5	9.09	−11.2 ± 3.5
3.39	−16.0 ± 3.6	2.03	−3.3 ± 2.0	3.05	−15.5 ± 2.1	6.26	−41.2 ± 3.9	6.59	−13.9 ± 6.1
2.98	−14.7 ± 3.7	1.77	−3.4 ± 0.5	2.65	−9.8 ± 2.2	7.12	−36.0 ± 5.5		
2.63	−8.1 ± 2.7	1.55	−1.9 ± 1.8	2.48	−8.6 ± 0.2	6.03	−33.4 ± 2.3		
2.53	−6.4 ± 1.5	5.79	−22.6 ± 3.9	1.99	−6.1 ± 3.6	6.47	−44.8 ± 7.2		
2.28	−5.4 ± 1.0	8.78	−22.6 ± 1.8	5.52	−26.4 ± 3.3	7.03	−43.8 ± 3.1		
5.85	−36.6 ± 4.8	9.09	−24.2 ± 2.3	5.97	−28.3 ± 4.8	7.83	−39.7 ± 2.4		
6.26	−36.4 ± 5.7	9.46	−20.8 ± 4.4	6.38	−34.6 ± 1.1	8.84	−30.4 ± 4.2		
6.91	−34.7 ± 2.6	10.00	−24.1 ± 4.9	6.64	−29.8 ± 8.7	9.49	−27.4 ± 2.2		
9.82	−38.0 ± 1.7	10.97	−28.0 ± 2.4	7.38	−35.7 ± 6.7	10.49	−29.2 ± 8.3		
10.37	−44.7 ± 1.3			7.97	−33.5 ± 3.4				
				9.44	−37.1 ± 4.9				
				10.57	−38.7 ± 0.2				

Uncertainty on pH is ±0.01 U.

Appendix D

See Table A4

Table A3
Experimental surface charge density of heated phytoliths as a function of pH, at 25 °C

$I = 0.01$ M		$I = 0.05$ M		$I = 0.5$ M	
pH	Si sites density (μmol/m^2)	pH	Si sites density (μmol/m^2)	PH	Si sites density (μmol/m^2)
Experimental datas on heated phytoliths titration, 20 g/L, 6.51 m^2/g, N_2 bubbling					
4.240	0.195	4.24	0.194	4.318	0.400
4.444	0.117	4.409	0.146	4.444	0.307
4.641	0.051	4.546	0.122	4.620	0.196
4.851	0.007	4.709	0.118	4.770	0.126
5.004	−0.027	4.832	0.115	4.897	0.070
5.177	−0.065	4.963	0.110	5.051	0.014
5.329	−0.109	5.090	0.098	5.125	−0.045
5.543	−0.184	5.255	0.084	5.383	−0.161
5.655	−0.229	5.378	0.054	5.416	−0.214
5.910	−0.314	5.535	−0.002	5.449	−0.262
5.994	−0.355	5.727	−0.068	5.566	−0.360
6.223	−0.436	5.782	−0.119	5.640	−0.439
6.305	−0.479	5.897	−0.180	5.852	−0.637
6.514	−0.561	6.012	−0.245	5.962	−0.746
6.614	−0.612	6.115	−0.316	6.031	−0.880
6.812	−0.710	6.293	−0.440	6.297	−1.154
6.953	−0.791	6.384	−0.523	6.247	−1.239
7.145	−0.913	6.614	−0.729	6.416	−1.419
7.321	−1.036	6.688	−0.830	6.378	−1.515
7.480	−1.172	6.884	−1.042	6.438	−1.602
7.609	−1.365	6.844	−1.126	6.538	−1.738
7.836	−1.674	6.817	−1.189	6.557	−1.911
7.944	−1.899	6.980	−1.362	6.605	−2.005
8.107	−2.261	7.024	−1.440	6.700	−2.147
8.236	−2.600	7.148	−1.600	6.707	−2.330
8.345	−2.936	7.131	−1.712	6.717	−2.443
8.441	−3.269	7.117	−1.793	6.855	−2.649
8.523	−3.601	7.266	−1.980	6.822	−2.774
		7.232	−2.058	6.860	−2.913
		7.316	−2.165	7.019	−3.166
		7.309	−2.265	6.998	−3.336
		7.356	−2.348	7.060	−3.459
		7.455	−2.481	7.062	−3.640
		7.445	−2.608	7.133	−3.775
		7.495	−2.699	7.127	−3.931
		7.507	−2.828	7.198	−4.064
		7.541	−2.957	7.193	−4.224
		7.656	−3.262	7.208	−4.376
		7.738	−3.541	7.277	−4.664
		7.979	−4.199	7.365	−5.029
		8.025	−4.518	7.506	−5.589
		8.053	−4.751	7.613	−6.117
		8.161	−5.211	7.784	−6.898
		8.231	−5.600	7.872	−7.506
		8.413	−6.368	8.001	−8.293
		8.480	−6.842	8.103	−9.058
		8.650	−7.709	8.203	−9.852
				8.294	−10.647
				8.375	−11.444
				8.453	−12.239
				8.521	−13.037
				8.592	−13.827
				8.659	−14.615

Table A4
X-ray photoelectron spectroscopy (XPS) analysis of different phytoliths

Element	Energy (eV)	Percent (%)	Atomic ratio: element/Si
"Soil" phytoliths			
C-1s	292.8	38.2	1.60
O-1s	541.1	38.0	1.59
Si-2s	162.9	23.8	1.00
"Heated" phytoliths			
C-1s	294.4	19.4	0.58
O-1s	542.5	47.0	1.40
Si-2s	164.2	33.6	1.00
"Heated" and grinded phytoliths			
C-1s	294.6	19.0	0.64
O-1s	542.8	51.3	1.73
Si-2s	164.3	29.7	1.00

References

Alexandre, A., Meunier, J.-D., Colin, F., Koud, J.M., 1997. Plant impact on the biogeochemical cycle of silicon and related weathering processes. *Geochim. Cosmochim. Acta* **61**, 677–682.

Allison, J.D., Brown, D.S., Novo-Gradac, K.J., 1991. MINTEQA2/PRODEFA2, A Geochemical Assessment Model for Environmental Systems: Version 3.0 User's Manual. U.S. EPA, Athens, GA, p. 106.

Bartoli, F., 1981. Le cycle biogéochimique du silicium sur roches acides. Application à deux systèmes forestiers tempérés. Thèse de Doctorat, Université de Nancy I, p. 187.

Bartoli, F., 1985. Crystallochemistry and surface properties of biogenic opal. *J. Soil Sci.* **36**, 335–350.

Brady, P.V., Walther, J.V., 1990. Kinetics of quartz dissolution at low temperatures. *Chem. Geol.* **82**, 253–264.

Busey, R.H., Mesmer, R.E., 1977. Ionisation equilibria of silic acid and polysilicate formation in aqueous sodium chloride solution to 300 °C. *Inorg. Chem.* **16**, 2444–2450.

Derry, L.A., Kurtz, A.C., Ziegler, K., Chadwick, O.A., 2005. Biological control of terrestrial silica cycling and export fluxes to watersheds. *Nature* **433**, 728–731.

Dixit, S., Van Cappellen, P., 2002. Surface chemistry and reactivity of biogenic silica. *Geochim. Cosmochim. Acta* **66**, 2559–2568.

Dove, P.-M., 1996. Kinetic and thermodynamic controls on silica reactivity in weathering environments. In: White, A.-F., Brantley, S.L. (Eds.), *Chemical Weathering Rates of Silica Minerals. Rev. Mineral.*, vol. 31, pp. 235–290.

Dove, P.-M., Elston, S.-F., 1992. Dissolution kinetics of quartz in sodium chloride solutions: analysis of existing data and a rate model for 25 °C. *Geochim. Cosmochim. Acta* **56**, 4147–4156.

Duval, Y., Mielczarski, J.A., Pokrovsky, O.S., Mielczarski, E., Ehrhardt, J.J., 2002. Evidence of the existence of three types of species at the quartz–aqueous solution interface at pH 0–10: XPS surface group quantification and surface complexation modeling. *J. Phys. Chem. B* **106**, 2937–2945.

Gautier, J.M., Oelkers, E.H., Schott, J., 2001. Are quartz dissolution rates proportional to BET surface areas? *Geochim. Cosmochim. Acta* **65**, 1059–1070.

Gélabert, A., Pokrovsky, O.S., Schott, J., Boudou, A., Feurtet-Mazel, A., Mielczarski, J., Mielczarski, E., Mesmer-Dudons, N., Spalla, O., 2004. Study of diatom/aqueous solution interface. I. Acid–base equilibria and spectroscopic observation of freshwater and marine species. *Geochim. Cosmochim. Acta* **68**, 4039–4058.

Goyne, K.W., Zimmerman, A.R., Newalkar, B.L., Komarneni, S., Brantley, S.L., Chorover, J., 2002. Surface charge of variable porosity Al_2O_3(s) and SiO_2(s) adsorbents. *J. Porous Mat.* **9**, 243–256.

Gun'ko, V.M., Mironyuk, I.F., Zarko, V.I., Voronin, E.F., Turov, V.V., Pakhlov, E.M., Goncharuk, E.V., Nychiporuk, Y.M., Vlasova, N.N., Gorbik, P.P., Mishchuk, O.A., Chuiko, A.A., Kulik, T.V., Pal-

yanytsya, B.B., Pakhovchishin, S.V., Skubiszewska-Zieba, J., Janusz, W., Turov, A.V., Leboda, R., . Morphology and surface properties of fumed silicas. *J. Colloid Interface Sci.* **289**, 427–445.

Guy, C., Schott, J., 1989. Multisite surface reaction versus transport control during the hydrolysis of a complex oxide. *Chem. Geol.* **78**, 181–204.

Herbelin, A.L., Westall, J.C., 1996. FITEQL Version 3.2, a Computer Program for Determination of Chemical Equilibrium Constants from Experimental Data. Department of Chemistry, Oregon State University. Corvallis, Oregon 97331.

Hiemstra, T., Van Riemsdijk, W.H., 1990. Multiple activated complex dissolution of metal (hydr)oxides: a thermodynamical approach applied to quartz. *J. Colloid Interface Sci.* **136**, 132–150.

Hiemstra, T., Venema, P., Van Riemsdijk, W.H., 1996. Intrinsic proton affinity of reactive surface groups of metal (hydr)oxides: the bond valence principle. *J. Colloid Interface Sci.* **184**, 680–682.

Hunter, R.J., 1989. *Foundation of Colloid Science*, vol. 1, Clarendon Press, Oxford.

Kelly, E.F., 1990. *Methods for Extracting Opal Phytoliths from Soil and Plant Material*: Fort Collins, Colorado State University, Department of Agronomy, Internal Document, p. 10.

Knauss, K.G., Wolery, T.J., 1988. The dissolution kinetics of quartz as a function of pH and time at 70 °C. *Geochim. Cosmochim. Acta* **52**, 43–53.

Koretsky, C.M., Sverjensky, D.A., Salisbury, J.W., D'Aria, D.M., 1997. Detection of surface hydroxyl species on quartz and feldspars using reflectance infrared spectroscopy. *Geochim. Cosmochim. Acta* **61**, 2193–2210.

Kosmulski, M., Maczka, E., Janusz, W., Rosenholm, J.B., 2002. Multi-instrument study of the electrophoretic mobility of quartz. *J. Colloid Interface Sci.* **250**, 99–103.

Li, H.C., De Bruyn, P.L., 1966. Electrokinetic and adsorption studies on quartz. *Surface Sci.* **5**, 203–220.

Lyklema, J., Rovillard, S., De Coninck, J., 1998. Electrokinetics: the properties of the stagnant layer unraveled. *Langmuir* **14**, 5659–5663.

Mackenzie, F.T., Garrels, R.M., 1966a. Chemical mass balance between rivers and oceans. *Am. J. Sci.* **264**, 507–525.

Mackenzie, F.T., Garrels, R.M., 1966b. Silica-bicarbonate balance in the ocean and early diagenesis. *J. Sed. Petrol.* **36**, 1075–1084.

Meunier, J.-D., Alexandre, A., Colin, F., et Braun, J.-J., 2001. Intérêt de l'étude du cycle du silicium pour interpréter la dynamique des sols tropicaux. *Bull. Soc. géol. Fr.* **172**, 533–538.

Meunier, J.-D., Colin, F., et Alarcon, C., 1999. Biogenic silica storage in soils. *Geology* **27**, 835–838.

Navrotsky, A., 1994. *Physics and Chemistry of Earth Materials*. Cambridge University Press, Cambridge, p. 417.

Piperno, D.R., 1988. *Phytolith. An Archaeological and Geological Perspective*. Academic Press, London, p. 280.

Pokrovsky, O.S., Savenko, V.S., 1992. Experimental determination of magnesium activity coefficient in seawater. *Oceanology* **32**, N6, 724–730.

Pokrovsky, O.S., Savenko, V.S., 1996. The total activity coefficient of calcium in seawater. *Oceanology* **36**, N1, 50–53.

Pokrovsky, O.S., Schott, J., Thomas, F., 1999. Processes at the magnesium-bearing carbonates/solution interface. I. A surface speciation model of magnesite. *Geochim. Cosmochim. Acta* **63**, 863–880.

Pokrovsky, O.S., Schott, J., 2000. Forsterite surface composition in aqueous solutions: a combined potentiometric, electrokinetic, and spectroscopic approach. *Geochim. Cosmochim. Acta* **64**, 3299–3312.

Pokrovsky, O.S., Schott, J., 2004. Experimental study of brucite dissolution and precipitation in aqueous solutions: surface speciation and chemical affinity control. *Geochim. Cosmochim. Acta* **68**, 31–45.

Pokrovsky, O.S., Golubev, S.V., Mielczarski, J.A., 2006. Kinetic evidence of the existence of positively charged species at the quartz–aqueous solution interface. *J. Colloid Interface Sci.* in press.

Pokrovsky, O.S., Schott, J., Dupré, B., Kudryavtzev, D.I., 2005. Basalts weathering in Central Siberia under permafrost conditions. *Geochim. Cosmochim. Acta* **69**, 5659–5680.

Rimstidt, J.D., Barnes, H.L., 1980. The kinetics of silica–water reactions. *Geochim. Cosmochim. Acta* **44**, 1683–1699.

Schott, J., 1990. Modelling of the dissolution of strained and unstrained multiple oxides: the surface speciation approach. In: Stumm, W. (Ed.), *Aquatic Chemical Kinetics: Reaction Rates of Processes in Natural Waters*. John Wiley & Sons, New York, pp. 337–365.

Schott, J., Pokrovsky, O.S., Spalla, O., Devreux, F., Mielczarski, J.A., 2002. The mechanism of altered layers formation on wollastonite revisited: a combined spectroscopic/kinetic study. Abstracts of the VM Goldschmidt Conference. August 18–23, Davos, Switzerland. Supplement to *Geochimica et Cosmochimica Acta*, 2002, p. A686.

Sillén, L.G., 1961. The physical chemistry of sea water. In: Sears, M. (Ed.), *Oceanography, Am. Assoc. Adv.* Pub. 67, pp., 549–581.

Stumm, W., 1992. *Chemistry of the Solid–Water Interface*. John Wiley & Sons, NewYork, p. 428.

Sverjensky, D.A., Sahai, N., 1996. Theoretical prediction of single-site surface-protonation equilibrium constants for oxides and silicates in water. *Geochim. Cosmochim. Acta* **60**, 3773–3797.

Van der Wal, A., Norde, W., Zehnder, A.J.B., Lyklema, J., 1997. Electrokinetic potential of bacterial cells. *Langmuir* **13**, 165–171.

Wilson, W.W., Wade, M.M., Holman, S.C., Champlin, F.R., 2001. Status of methods for assessing bacterial cell surface charge properties based on zeta potential measurements. *J. Microbiol. Methods* **43**, 153–164.

Wirth, G.S., Gieskes, J.M., 1979. The initial kinetics of the dissolution of vitreous silica in aqueous media. *J. Colloid Interface Sci.* **68**, 492–500.

Wollast, R., Mackensie, F.T., 1983. The global cycle of silica. In: Aston, S.R. (Ed.), *Silicon Geochemistry and Biogeochemistry*. Academic press, San Diego, pp. 39–76.

Xu, G., Zhang, J., Song, G., 2003. Effect of complexation on the zeta potential of silica powder. *Powder Technol.* **134**, 218–222.